



Characterization of the Reconstructed 1918 Spanish Influenza Pandemic Virus

Terrence M. Tumpey, *et al.*

Science **310**, 77 (2005);

DOI: 10.1126/science.1119392

The following resources related to this article are available online at www.sciencemag.org (this information is current as of February 3, 2009):

Updated information and services, including high-resolution figures, can be found in the online version of this article at:

<http://www.sciencemag.org/cgi/content/full/310/5745/77>

Supporting Online Material can be found at:

<http://www.sciencemag.org/cgi/content/full/310/5745/77/DC1>

A list of selected additional articles on the Science Web sites **related to this article** can be found at:

<http://www.sciencemag.org/cgi/content/full/310/5745/77#related-content>

This article **cites 21 articles**, 17 of which can be accessed for free:

<http://www.sciencemag.org/cgi/content/full/310/5745/77#otherarticles>

This article has been **cited by** 194 article(s) on the ISI Web of Science.

This article has been **cited by** 61 articles hosted by HighWire Press; see:

<http://www.sciencemag.org/cgi/content/full/310/5745/77#otherarticles>

This article appears in the following **subject collections**:

Virology

<http://www.sciencemag.org/cgi/collection/virology>

Information about obtaining **reprints** of this article or about obtaining **permission to reproduce this article** in whole or in part can be found at:

<http://www.sciencemag.org/about/permissions.dtl>

Characterization of the Reconstructed 1918 Spanish Influenza Pandemic Virus

Terrence M. Tumpey,^{1*} Christopher F. Basler,²
 Patricia V. Aguilar,² Hui Zeng,¹ Alicia Solórzano,²
 David E. Swayne,⁴ Nancy J. Cox,¹ Jacqueline M. Katz,¹
 Jeffery K. Taubenberger,³ Peter Palese,² Adolfo García-Sastre²

The pandemic influenza virus of 1918–1919 killed an estimated 20 to 50 million people worldwide. With the recent availability of the complete 1918 influenza virus coding sequence, we used reverse genetics to generate an influenza virus bearing all eight gene segments of the pandemic virus to study the properties associated with its extraordinary virulence. In stark contrast to contemporary human influenza H1N1 viruses, the 1918 pandemic virus had the ability to replicate in the absence of trypsin, caused death in mice and embryonated chicken eggs, and displayed a high-growth phenotype in human bronchial epithelial cells. Moreover, the coordinated expression of the 1918 virus genes most certainly confers the unique high-virulence phenotype observed with this pandemic virus.

The influenza pandemic of 1918 was exceptional, resulting in the deaths of up to 50 million people worldwide, including an estimated 675,000 deaths in the United States (1, 2). The pandemic's most striking feature was the unusually high death rate among healthy adults aged 15 to 34 years, which consequently lowered the average life expectancy in the United States by more than 10 years (3). A similarly high death rate has not occurred in this age group in either prior or subsequent influenza A pandemics or epidemics (4).

Genomic RNA of the 1918 virus was recovered from archived formalin-fixed lung autopsy materials and from frozen, unfixed lung tissues from an Alaskan influenza victim who was buried in permafrost in November of 1918 (5, 6). The complete coding sequences of all eight viral RNA segments have now been determined, and analysis of these sequences has provided insights into the nature and origin of this pathogen (5–11). Plasmid-based reverse genetics has allowed for the generation of recombinant viruses containing 1918 hemagglutinin (HA) with or without the 1918 neuraminidase (NA) rescued in the genetic background of contemporary

human H1N1 or H3N2 influenza viruses. The resulting strains were demonstrated to cause mortality in mice only at high infection doses (12, 13); however, the virulence of the complete 1918 virus has not been evaluated.

In the present study, we generated a virus containing the complete coding sequences of the eight viral gene segments from the 1918 virus in an effort to understand the molecular basis of virulence of this pandemic virus. Genes encoding the 1918 influenza virus were reconstructed from deoxyoligonucleotides and corresponded to the reported coding sequences of the 1918 virus as previously described (5–11). Because the 1918 5' and 3' noncoding regions have not been sequenced, the genes were constructed such that they had the noncoding regions corresponding to the closely related influenza A/WSN/33 (H1N1) virus. The 1918 virus and recombinant H1N1 influenza viruses were generated using the previously described reverse genetics system (8, 14). All viruses containing one or more gene segments from the 1918 influenza virus were generated and handled under high-containment [biosafety level 3 enhanced (BSL3)] laboratory conditions in accordance with guidelines of the National Institutes of Health and the Centers for Disease Control and Prevention (15). Viruses were grown in Madin-Darby canine kidney cells (MDCK) cells and/or the allantoic cavity of 10-day-old embryonated hens' eggs (table S1). The control viruses included an avian A/duck/Alberta/35/76 H1N1 virus, two contemporary human H1N1 influenza viruses, the wild-type A/New Caledonia/20/99 (N. Cal/99, H1N1) virus and A/Texas/36/91 (Tx/91, H1N1) virus generated by reverse genetics. The other recombinant viruses used were a virus having only

the HA from the Tx/91 virus with the remaining seven genes from the 1918 virus (Tx/91 HA:1918); a virus having the NA from 1918 with the remaining seven genes from the Tx/91 virus (1918 NA:Tx/91); and recombinant viruses having two 1918 (1918 HA/NA:Tx/91) or five 1918 genes (1918 HA/NA/NP/NS:Tx/91) with the remaining genes derived from the Tx/91 virus. The HA of the 1918 viruses used throughout these studies was derived from A/South Carolina/1/18 strain that was shown to preferentially bind the α 2,6 sialic acid (human) cellular receptor (16). The identity of the 1918 and Tx/91 influenza virus genes in the rescued viruses was confirmed by reverse transcription polymerase chain reaction and sequence analysis.

The infectivity of the 1918 virus and the ability to form plaques in the presence and in the absence of the protease trypsin were assayed in MDCK cells by the plaque method. The proteolytic cleavage of the HA molecule is a prerequisite for multicycle replication, and the ability of an influenza virus to replicate in the absence of trypsin has been thought to be an important determinant of influenza virus pathogenicity in mammals (17–20). In contrast to the contemporary human Tx/91 and N. Cal/99 H1N1 viruses, which require an exogenous protease source for their multicycle replication and plaque formation (Table 1), the 1918 virus and a recombinant influenza virus bearing the 1918 HA and NA segments only (1918 HA/NA:Tx/91) formed visible plaques without the addition of trypsin (Table 1). Furthermore, a virus having only the 1918 NA with the remaining genes, including the HA, from Tx/91 virus (1918 NA:Tx/91) also replicated in the absence of trypsin, which suggests that the 1918 NA activity facilitates HA cleavage. However, the 1918 HA and NA gene sequences lack the obvious genetic features that have previously been associated with the ability

Table 1. Plaque formation of the 1918 virus in MDCK cells with or without trypsin. Serial 10-fold dilutions of virus stocks were prepared before a standard plaque assay. Duplicate monolayers of MDCK cells were washed extensively (7 times) before and after adsorption of virus. An agar overlay was added with or without trypsin (1 μ g/ml, Sigma) and incubated at 37°C with 5% CO₂ for 48 hours. 1918 (1) and (2) represent two independently rescued viruses.

Virus	Infectivity titer (PFU/ml)	
	Trypsin (+)	Trypsin (–)
N. Cal/99	3.6×10^7	–*
Tx/91	1.4×10^7	–
1918 HA/NA:Tx/91	2.4×10^7	2.1×10^7
1918 NA:Tx/91	3.4×10^7	2.5×10^7
1918 (1)	4.8×10^7	4.2×10^7
1918 (2)	1.4×10^8	1.1×10^8

*No visible plaques were formed at the lowest dilution (1:10) tested.

¹Influenza Branch, Mailstop G-16, Division of Viral and Rickettsial Diseases (DVRD), National Center for Infectious Diseases, Centers for Disease Control and Prevention, 1600 Clifton Road, NE, Atlanta, GA 30333, USA. ²Department of Microbiology, Mount Sinai School of Medicine, New York, NY 10029, USA. ³Department of Molecular Pathology, Armed Forces Institute of Pathology, Rockville, MD 20850, USA. ⁴Southeast Poultry Research Laboratory, Agricultural Research Laboratory (ARS), U.S. Department of Agriculture (USDA), 934 College Station Road, Athens, GA 30606, USA.

*To whom correspondence should be addressed. E-mail: tft9@cdc.gov

to replicate in the absence of trypsin; that is, the 1918 virus has neither a series of basic amino acids at the HA cleavage site (as seen in highly pathogenic avian H5 or H7 influenza viruses) nor mutations (N146R or N146Y) in the NA that lead to the loss of a glycosylation site like those that allow the A/WSN/33 virus NA to sequester plasminogen (6, 7, 17, 18, 20). We will need to consider other mechanisms of NA-mediated HA cleavability that may be relevant to the replication and virulence of the 1918 virus.

To evaluate the pathogenicity of the 1918 virus in a mammalian species, we intranasally inoculated BALB/c mice with two independently generated 1918 viruses and then determined morbidity (measured by weight loss), virus replication, and 50% lethal dose (LD_{50}) titers (21, 22). For comparison, groups of mice were infected with a recombinant influenza virus containing five 1918 genes with the remaining three polymerase genes from Tx/91 (1918 HA/NA/M/NP/NS:Tx/91) virus or a recombinant 1918 virus (Tx/91 HA:1918), in which the HA has been replaced with that of Tx/91 virus. Infection of mice with the 1918 virus resulted in lung virus titers, on day 4 post inoculation (p.i.), that were at least 125 and 39,000 times those of mice infected with the Tx/91 HA:1918 and Tx/91 viruses, respectively (Fig. 1A). The 1918 HA/NA/M/NP/NS:Tx/91 virus also replicated efficiently in the mouse lung, but virus titers were markedly lower than those for mice infected with the 1918 virus, and the lethality of the 1918 virus ($LD_{50} = 10^{3.25-3.5}$) was at least 100 times that for the 1918 HA/NA/M/NP/NS:Tx/91 virus ($LD_{50} = 10^{5.5}$). Strikingly, the mice infected with 10^6 PFU (plaque-forming units) of the 1918 virus succumbed to infection as early as 3 days p.i. (Fig. 1B), and they lost up to 13% of their body weight 2 days after infection (Fig. 1C). In contrast to the lethal outcome of the 1918 virus infection, the Tx/91 HA:1918 virus, like the

wild-type Tx/91 virus, did not kill mice ($LD_{50} = 10^{>6}$) (Fig. 1B) and displayed only transient weight reduction (Fig. 1C). To determine whether the 1918 virus replicated systemically in the mouse after intranasal infection with 10^6 PFU of virus, we harvested brain, heart, liver, and spleen tissues from four mice each on days 4 and 5 p.i. All eight mice infected with the 1918 virus or the Tx/91 control viruses had undetectable levels [$\leq 10^{0.8}$ of the 50% egg infectious dose (EID_{50})/ml determined by serial titration in chicken eggs] of virus in these tissues (fig. S1), which indicated that the 1918 virus did not spread systemically to other organs in the mouse.

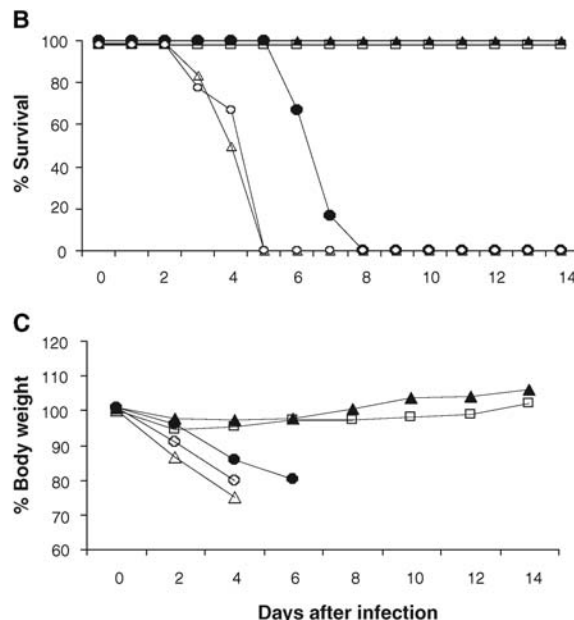
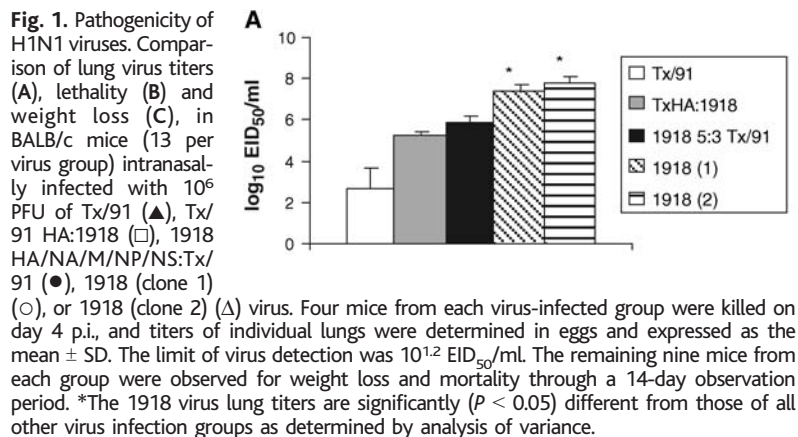
Histopathological analysis of lung tissues from individuals who died from primary influenza pneumonia in 1918 frequently showed acute pulmonary edema and/or hemorrhage with acute bronchiolitis, alveolitis, and bronchopneumonia (23). In mice, the most severe lung lesions were observed after infection with the 1918 virus (21). On day 4 p.i., mice infected with the pandemic strain had necrotizing bronchitis and bronchiolitis and moderate to severe alveolitis (Fig. 2A). The alveolitis varied from peribron-

chial to diffuse in distribution and was composed of neutrophils and macrophages. Accompanying the inflammation was moderate-to-severe peribronchial and alveolar edema (Fig. 2B) and alveolar hemorrhage. Neutrophils were the predominant inflammatory cells, but alveolar macrophages were also prominent (Fig. 2C). As in autopsy studies performed in 1918, there was no histological evidence of systemic infection such as necrosis or inflammation in the liver, kidney, spleen, heart, and brain tissues of mice infected with the 1918 virus. In general, the 1918 HA/NA/M/NP/NS:Tx/91 virus induced less severe pathology; however, mild-to-moderate peribronchial alveolitis with some mild-to-moderate alveolar edema was observed (Fig. 2D). The 1918 HA gene was essential for severe pulmonary lesion development, because the Tx/91 HA:1918 virus produced very mild pulmonary lesions characterized by minimal, diffuse alveolitis and mild focal lymphocytic-histiocytic peribronchitis (Fig. 2E). The Tx/91-inoculated mice lacked noteworthy lesions in the lungs (Fig. 2E).

Since 1918 virus gene sequences are related more closely to avian H1N1 viruses than any

Table 2. Lethality of the 1918 influenza virus for 10-day-old embryonated chicken eggs. Fifty percent egg infectious dose (EID_{50}) and egg lethal dose (ELD_{50}) titers were determined as described in the text. For ELD_{50} titers, embryo viability was visually determined by daily candling. EID_{50} and ELD_{50} titers were determined simultaneously and calculated by the method of Reed and Muench (27). The mean death time (MDT) of embryo death was calculated by examining embryo viability daily for 7 days. The MDT is the mean time in days for the minimum lethal dose to kill embryos.

Virus	$\log_{10} EID_{50}/ml$	$\log_{10} ELD_{50}/ml$	MDT (day)
N. Cal/99	8.5	≤ 1.2	-
Tx/91	8.7	≤ 1.2	-
Tx/91 HA:1918	9.0	≤ 1.2	-
1918 HA/NA:Tx/91	9.0	≤ 1.2	-
1918 HA/NA/M/NP/NS:Tx/91	8.7	≤ 1.2	-
1918 (1)	9.0	7.2	4.5
1918 (2)	9.5	8.2	4.5
A/duck/Alberta/35/76	9.0	8.5	2



other mammalian H1N1 strains (5–11), it was of interest to determine whether the 1918 strain would be lethal for fertile chicken eggs, a pathogenic feature of avian H1N1 viruses. After serial titration in 10-day-old embryonated chicken eggs, the 1918 virus was lethal for chicken embryos: 50% egg lethal dose (ELD₅₀) titers

were similar to those for an avian H1N1 representative, A/duck/Alberta/35/76 virus (Table 2). By contrast, neither contemporary human H1N1 viruses nor any of the 1918 recombinant viruses containing two, five, or seven genes from the 1918 virus caused mortality of embryos by day 7 p.i., which indicated that the 1918 HA

and 1918 polymerase genes were associated with virulence of chicken embryos.

We evaluated growth and release of the virus in polarized Calu-3 cells, a human lung epithelial cell line, grown on membrane inserts (24). Culture medium was collected from the apical and basolateral chambers at different times after inoculation and examined for virus production in the presence or absence of trypsin. With all viruses tested, titers of progeny virus progressively increased during the first 24 hours p.i., and virus was detected almost exclusively in the apical supernatant (Fig. 3). Regardless of the presence or absence of trypsin, infectivity titers of the 1918 virus were significantly higher than virus titers released in the Tx/91 HA:1918 and 1918 HA/NA/M/NP/NS:Tx/91 virus-infected cultures at 12, 16 and 24 hours p.i., which suggests that the 1918 HA and 1918 polymerase genes are essential for maximal replication of the virus in human bronchial epithelial cells. At 16 and 24 hours p.i., 1918 virus release was at least 50 times that observed in Tx/91 virus-infected cultures. The evidence of significantly higher apical release of 1918 progeny virus after an apical infection supports the hypothesis of an increase in the amount of virus present in the infected lung and may provide important insight into the virulence of this virus.

Until now, the exceptional virulence of the 1918 pandemic influenza virus has been a question of historical curiosity. Herein, we demonstrate the successful reconstruction of the 1918 pandemic virus in order to understand more fully the virulence of this virus and possibly of other human influenza pandemic viruses. Because the emergence of another pandemic virus is considered likely, if not inevitable (25), characterization of the 1918 virus may enable us to recognize the potential threat posed by new influenza virus strains, and it will shed light on the prophylactic and therapeutic countermeasures that will be needed to control pandemic viruses. A number of biological properties associated with this unusually virulent influenza virus were found. Comparison of the 1918 virus with recombinant viruses expressing one or more 1918 virus genes demonstrated that the 1918 HA and polymerase genes are essential for optimal virulence

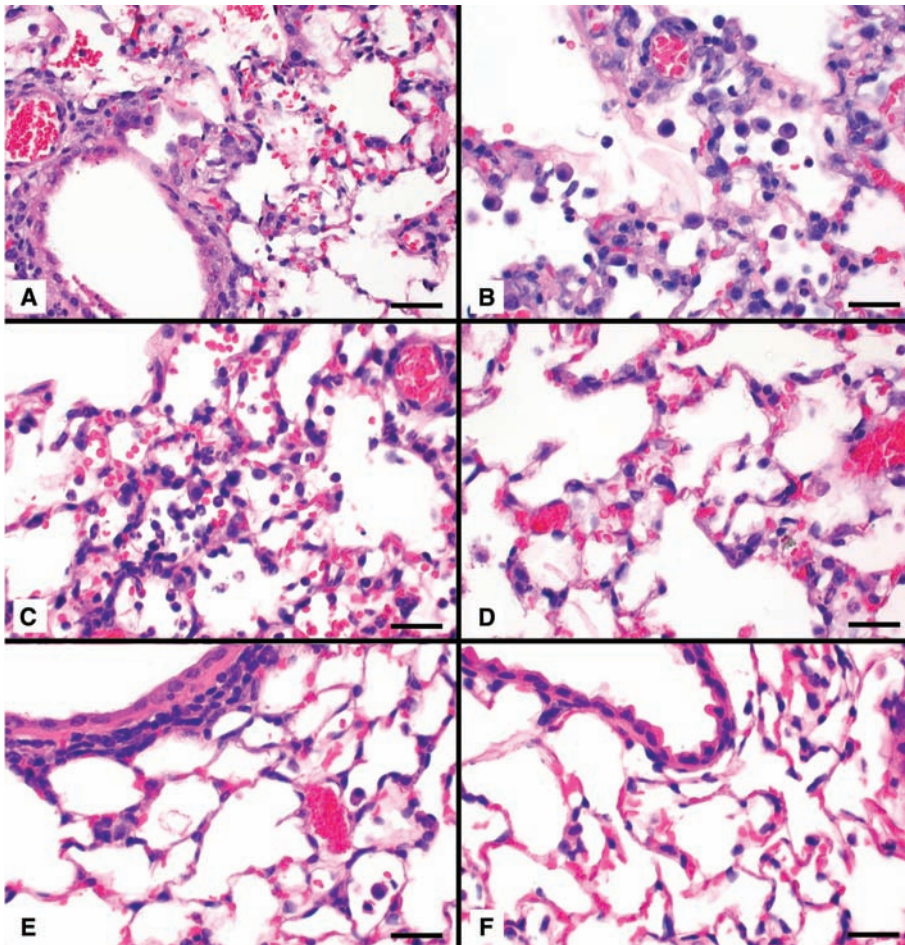
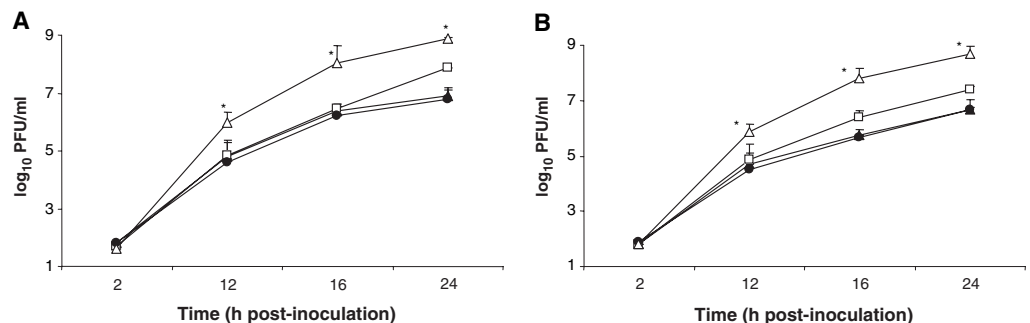


Fig. 2. Photomicrographs of hematoxylin and eosin-stained lung sections. (A to C), lungs from mice infected with the 1918 influenza virus: (A) necrotizing bronchiolitis and severe alveolitis, (B) severe alveolar edema and histiocytic alveolitis with scattered neutrophils, and (C) alveolitis, predominantly neutrophilic, and associated hemorrhage. (D) Moderate alveolitis and edema in lungs from a mouse infected with 1918 HA/NA/M/NP/NS:Tx/91 virus. (E) Mild peribronchial inflammation with adjacent minimal alveolitis in a mouse infected with Tx/91 HA:1918 virus. (F) Lung tissue from a Tx/91-infected mouse showing the paucity of lesions. Scale bars, 25 μ m (A) and 15 μ m (B to F).

Fig. 3. Release of 1918 influenza virus from apically infected human bronchial epithelial cells. Calu-3 cells were grown to confluency on transwell inserts as previously described (24). Cells were infected with Tx/91 (\blacktriangle), Tx/91 HA:1918 (\square), 1918 HA/NA/M/NP/NS:Tx/91 (\bullet), or 1918 (\triangle) virus at an MOI of 0.01 for 1 hour at 37°C. Unbound virus was removed by washing the cells 3 times, and infected cells were cultured in Dulbecco's modified Eagle's medium (DMEM) medium supplemented with 0.3% bovine serum albumin in the presence (A) or absence (B) of trypsin (1 μ g/ml; Sigma, St. Louis, MO). Apical and basolateral (not shown) supernatants were collected at the indicated times and virus content was determined in a standard plaque assay.



The values shown represent the mean virus titer of fluids from three replicate infected cultures. *The 1918 virus titers are significantly ($P < 0.05$) different from those of all other virus infection groups as determined by analysis of variance.

and that the constellation of all eight genes together make an exceptionally virulent virus in the model systems examined. In fact, no other human influenza viruses that have been tested show a similar pathogenicity for mice 3 to 4 days after infection. This information provides a partial explanation for what made this virus so lethal. In this regard, it should be noted that the U.S. Food and Drug Administration (FDA)-approved antiviral drugs, oseltamivir and amantadine, have been shown to be effective against viruses carrying the 1918 NA and the 1918 M gene, respectively (22). Furthermore, vaccines containing the 1918 HA and NA were protective in mice (26).

Note added in proof: This research was done by staff taking antiviral prophylaxis and using stringent biosafety precautions (15) to protect the researchers, the environment, and the public. The fundamental purpose of this work was to provide information critical to protect public health and to develop measures effective against future influenza pandemics.

REPORTS

A Reversible, Unidirectional Molecular Rotary Motor Driven by Chemical Energy

Stephen P. Fletcher, Frédéric Dumur, Michael M. Pollard, Ben L. Feringa*

With the long-term goal of producing nanometer-scale machines, we describe here the unidirectional rotary motion of a synthetic molecular structure fueled by chemical conversions. The basis of the rotation is the movement of a phenyl rotor relative to a naphthyl stator about a single bond axle. The sense of rotation is governed by the choice of chemical reagents that power the motor through four chemically distinct stations. Within the stations, the rotor is held in place by structural features that limit the extent of the rotor's Brownian motion relative to the stator.

One of the most challenging components required for the fabrication of molecular machines (1–5) is the rotary motor (6, 7): the element that converts energy into controlled rotational motion (8). Natural systems often use adenosine triphosphate (ATP) as an energy source. Rotation in these systems is powered by the energy released upon the hydrolytic conversion of ATP to the diphosphate ADP (6, 9, 10). The system introduced here analogously uses exothermic chemical reactions to power unidirectional rotary motion.

Department of Organic and Molecular Inorganic Chemistry, Stratingh Institute, University of Groningen, Nijenborgh 4, 9747 AG Groningen, Netherlands.

*To whom correspondence should be addressed. E-mail: b.l.feringa@chem.rug.nl

References and Notes

1. A. Crosby, *America's Forgotten Pandemic* (Cambridge Univ. Press, Cambridge, 1989).
2. N. P. Johnson, J. Mueller, *Bull. Hist. Med.* **76**, 105 (2002).
3. W. P. Glezen, *Epidemiol. Rev.* **18**, 64 (1996).
4. E. D. Kilbourne, in *The Influenza Viruses and Influenza*, E. D. Kilbourne, Ed. (Academic Press, New York, 1975), pp. 483–538.
5. J. K. Taubenberger *et al.*, *Science* **275**, 1793 (1997).
6. A. H. Reid *et al.*, *Proc. Natl. Acad. Sci. U.S.A.* **96**, 1651 (1999).
7. A. H. Reid *et al.*, *Proc. Natl. Acad. Sci. U.S.A.* **97**, 6785 (2000).
8. C. Basler *et al.*, *Proc. Natl. Acad. Sci. U.S.A.* **98**, 2746 (2001).
9. A. H. Reid *et al.*, *J. Virol.* **76**, 10717 (2002).
10. A. H. Reid *et al.*, *J. Virol.* **78**, 12462 (2004).
11. J. K. Taubenberger *et al.*, *Nature* **437**, 889 (2005).
12. D. Kobasa *et al.*, *Nature* **431**, 703 (2004).
13. T. M. Tumpey *et al.*, *J. Virol.*, in press.
14. E. Fodor *et al.*, *J. Virol.* **73**, 9679 (1999).
15. Interim CDC-NIH Recommendation (www.cdc.gov/flu/h2n2bs13.htm).
16. L. Glaser *et al.*, *J. Virol.* **79**, 11533 (2005).
17. H. Goto, Y. Kawaoka, *Proc. Natl. Acad. Sci. U.S.A.* **95**, 10224 (1998).
18. H. Goto *et al.*, *J. Virol.* **75**, 9297 (2001).
19. M. Hatta, P. Gao, P. Halfmann, Y. Kawaoka, *Science* **293**, 1840 (2001).
20. S. Li *et al.*, *J. Virol.* **67**, 6667 (1993).
21. Materials and methods are available as supporting material on Science Online.

22. T. M. Tumpey *et al.*, *Proc. Natl. Acad. Sci. U.S.A.* **99**, 13849 (2002).
23. M. C. Wintemitz, I. M. Wason, F. P. McNamara, *The Pathology of Influenza* (Yale Univ. Press, New Haven, CT, 1920).
24. C.-T. K. Tseng *et al.*, *J. Virol.* **79**, 9470 (2005).
25. R. J. Webby, R. G. Webster, *Science* **302**, 1519 (2003).
26. T. M. Tumpey *et al.*, *Proc. Natl. Acad. Sci. U.S.A.* **101**, 3166 (2004).
27. L. J. Reed, H. Muench, *Am. J. Hyg.* **27**, 493 (1938).
28. This work was partially supported by grants from the NIH to P.P., A.G.-S., C.F.B., and J.K.T. In the Ellison Medical Foundation Program in Global Infectious Diseases, P.P. is a Senior Fellow and C.F.B. is a New Scholar. This work was partially supported by USDA/ARS Current Research Information System (CRIS) project number 6612-32000-039-00D and by National Institute of Allergy and Infectious Diseases (NIAID) cooperative agreements with the Northeastern Biodefense Center (US4 A157158) and with the Center for Investigating Viral Immunity and Antagonism (CIVIA) (U19 AI62623), as well as by NIAID grant P01 AI058113-01.

Supporting Online Material

www.sciencemag.org/cgi/content/full/310/5745/77/DC1

Materials and Methods

Fig. S1

Table S1

References and Notes

26 August 2005; accepted 20 September 2005

10.1126/science.1119392

Purely chemical strategies have been scarcer (7, 20, 21). Limited unidirectional (120°) rotation about a single bond in a helically shaped molecule (22, 23) has been achieved with a modified molecular ratchet (24–26). Here, we report a system that uses chemical energy to achieve unidirectional 360° rotation of one half of the molecule relative to the other half (Fig. 1). The rotation is driven by a combination of chemical reactions and random thermal (Brownian) motion. Understanding these processes may be relevant to natural molecular motors, which work on similar principles.

Our system consists of a rotor half and a stator half, connected by a single carbon-carbon bond which acts as the axis of rotation (Fig. 1). Chemical reactions control movement of the rotor through four structurally distinct stations, with the net effect of turning the rotor 360° relative to the stator. Bonding and steric constraints limit the extent of the rotor's uncontrolled Brownian motion. In two of the stations (Fig. 1, stations A and C) the rotor's position is restricted by the action of additional chemical bonds, although helix inversion can occur. In stations B and D (Fig. 1), the rotor and stator cannot pass each other due to nonbonding interactions. Movement between the stations is guided by four power strokes, or chemically induced rotational events. The complete cycle involves two bond-breaking steps (step 1 and step 3) and two bond-making steps (step 2 and step 4), each of which provides the driving force for approximately 90° unidirectional rotation to the next station.

Two general mechanisms (27) for the conversion of energy into mechanical motion have